PHYSICAL REVIEW E **78**, 021904 (2008)

Charge density coordination and dynamics in a rodlike polyelectrolyte

Won Kyu Kim[*] and Wokyung Sung[†]
Department of Physics and PCTP, Pohang University of Science and Technology, Pohang 790-784, South Korea

(Received 14 March 2008; published 11 August 2008)

We study static and dynamic correlation functions of segmental charge density fluctuation on a rodlike polymer in ionic solutions. The polymer is described by an effective Hamiltonian which incorporates the Coulomb interaction between fluctuating charges screened by ionic fluid environment. We analytically calculate the correlation functions and discuss how charge distribution and dynamics are affected by counterion valency and concentration in electrolyte. We find that the charge correlation exhibits an underdamped oscillation with a wavelength comparable to the counterion size and with the amplitude increasing with the counterion valency. The dynamic correlation of charge density is shown to decay with a characteristic time varying with the counterion valency and concentration. The multivalency gives rise to faster decay of the correlation than that given by one dimensional diffusion.

DOI: 10.1103/PhysRevE.78.021904 PACS number(s): 87.15.Pc, 36.20.−r, 61.20.Qg

I. INTRODUCTION

The biopolymers such as DNA, RNA, actin filaments, microtubules, etc., play an important role in vital activities particularly in subcellular level as essential structures and functional agencies. One notable feature is that they carry charges, surrounded by electrolyte solution. The Manning-Oosawa counterion condensation theory [1,2] describes that the counterion absorption occurs above a critical charge density of the polyelectrolyte and has been a basis of the extensive studies that followed. It has been theoretically suggested [2–5] that the charge density fluctuations on the polymer induced by mobile condensed counterions can give rise to bundle formation [6–9] of like-charged polyelectrolytes as a result of van der Waals–like attraction: when close to each other, they can attract due to correlation of charge density fluctuations on each polymer [5]. The charge correlation also is responsible for DNA collapse [6,10,11] and related reduction of bending rigidity [12,13].

Also, by numerical simulations [14,15], charge oscillation on a rodlike polyelectrolyte has been observed in the pair correlation function of the condensed counterions, which is similar to the short-range order in a simple liquid. Notably, the counterion-induced charge fluctuation manifests oscillation along the polymer [5]. Recently, Angelini *et al.* observed counterion charge density waves (CDWs) between attracted F-actin filaments with small angle x-ray scattering (SAXS) [8].

Along with the spatial oscillations, counterion dynamics on the polymer, probed by time correlation function, is another important issue. By high-resolution inelastic x-ray scattering experiment [16], an acousticlike phonon mode of the CDW on a bundle of F-actin filaments was observed, yielding a nontrivial dynamics associated with cage effect of the ions. The phonon mode of the charge density was predicted by Zandt *et al.* also for a single DNA with counterions [17]. Recently, a molecular dynamics study [18] reported that the dynamical charge autocorrelation function on the polyelectrolyte condensed typically with monovalent counterions decays within 0.1 ns. But, analytical characterization of their dynamics and dependence on the counterion valency and ionic strength is still lacking. Furthermore, in spite of extensive studies for radial charge correlation functions of the polyelectrolyte, there have been only a few studies for both spatial (longitudinal) and temporal charge density fluctuations along the polymer.

In this paper, we investigate equilibrium distribution and dynamical behavior of the charge density on the rodlike polymer in an asymmetric electrolyte solution with screened Coulomb interaction in terms of the static and dynamic correlation functions. We interpret the correlation function by linear response theory, where it is proportional to charge density response to a perturbation on a neighboring position. In the following section, we consider a fluctuating charge density with a model Hamiltonian of the system described above. We find the correlation functions of the charge density show underdamped oscillation with a characteristic length of the oscillation directly associated with the size of the counterions. The amplitude of the correlation function depends on valency of the counterions and electrolyte concentration, which is analyzed. In Sec. III, we use a dynamical equation of motion for the charge fluctuation and obtain the time correlation functions. We discuss how the characteristic decay time depends on the valency and concentration. We show that the autocorrelation for the case of strong electrostatic interaction decays much faster than is given in one dimensional diffusion.

II. EFFECTIVE HAMILTONIAN AND STATIC CORRELATION

We consider that a negatively charged rodlike polymer of a length L is immersed in an ionic solution with no external flow. The solution is composed of monovalent anions and neutralizing cations of the valency of $z(\geqslant 1)$. The bare polymer is assumed to have a fixed number density, $\sigma_0 = 1/a$. a is a microscopic length which contains a negative elementary

---

[*] infinity@postech.ac.kr
[†] wsung@postech.ac.kr

charge $-e$. A DNA is a strongly charged polyelectrolyte with a known to be 0.17 nm.

Consider that the segmental position is given by s, the contour length along the chain, $0 \leqslant s \leqslant L$. Due to thermal fluctuation, the counterions will incessantly adsorb and desorb on the segments, constituting an effective line charge density $\sigma(s)$ that varies spatially and temporally [19]. Denoting its fluctuation by $\delta\sigma(s)[\sigma(s)=\langle\sigma\rangle+\delta\sigma(s)]$, the effective Hamiltonian of the rodlike polyelectrolyte is given as H:

$$\beta H = \frac{\chi}{2}\int_0^L ds[\delta\sigma(s)]^2 + \frac{l_B}{2}\int_0^L\int_0^L ds\,ds'\,\frac{\sigma(s)\sigma(s')}{|s-s'|}e^{-\kappa_D|s-s'|}, \tag{1}$$

where $\beta=1/k_BT$ and $l_B=e^2/(\varepsilon k_BT)$ is the Bjerrum length. The first term in Eq. (1) denotes the entropy cost for the charge fluctuation evaluated to the harmonic order. It means that, with the electrostatic interaction turned off, the charge density obeys a Gaussian distribution with the average $\langle\sigma\rangle$ and variance proportional to χ^{-1}. The last term in Eq. (1) is the screened Coulomb interaction with the Debye-Hückel screening length $\lambda_D=\kappa_D^{-1}=1/\sqrt{4\pi l_B z(z+1)c}$ for z:1 electrolyte and c is its concentration [20].

To evaluate the χ, a measure of inverse charge fluctuation, self-consistently, the charge density on the polymer is defined as $\sigma(s)=-\sigma_0+z\sigma_z(s)$ with $\sigma_z(s)=\langle\sigma_z\rangle+\delta\sigma_z(s)$, the number density of absorbed counterions, with e put to unity, so that $\langle\sigma\rangle=-\sigma_0+z\langle\sigma_z\rangle$ and $\delta\sigma(s)=z\delta\sigma_z(s)$. We consider the absorbed counterions under no electrostatic interactions as ideal gas and use the entropic contribution to free energy,

$$\beta F_{ent} = \int_0^L ds[\sigma_z(s)\ln(\sigma_z(s)l_0)-\sigma_z(s)], \tag{2}$$

where l_0 is a microscopic length. Expanding Eq. (2) to the harmonic order in $\delta\sigma$ and comparing it with Eq. (1), we obtain $\chi=1/(z^2\langle\sigma_z\rangle)$. For the average number density of absorbed counterions, $\langle\sigma_z\rangle$, we use the mean charge density, $\langle\sigma\rangle=-1/(l_Bz)$ following Manning-Oosawa mean field theory for a rodlike chain in the z:1 electrolyte [Eq. (3.10) in Ref. [20]]. It has been also shown that the $\langle\sigma\rangle$ is valid up to the z:1 electrolyte concentration as high as ~100 mM [21,22]. Then we obtain $\chi=al_B/(zl_B-a)$ which coincides with that in Ref. [12].

To facilitate evaluation of the charge density correlation functions, we analyze the Hamiltonian in the Fourier space using the Fourier mode of $\delta\sigma(s)$ defined as

$$\delta\sigma(s) = \frac{1}{\sqrt{L}}\sum_q e^{-iqs}\delta\sigma(q), \tag{3}$$

where $L=Nb$. Here N is the total number of the basic segment and b, to be determined later, is its length incorporating the effective charge. The q accordingly has N discrete values $q=2n\pi/L$ ranging from $-\pi/b$ to π/b with integer $n=-N/2,\ldots,N/2$. Then, to the harmonic order in the charge fluctuation modes, Eq. (1) is represented as

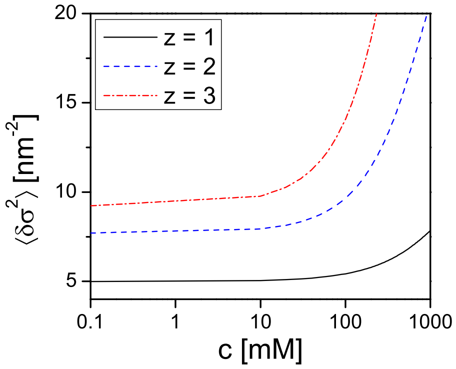

FIG. 1. (Color online) $\langle\delta\sigma^2\rangle$ as a function of c for various valency z.

$$\beta H = \frac{1}{2}\sum_q S^{-1}(q)|\delta\sigma(q)|^2, \tag{4}$$

where

$$S(q) = [\chi + 2l_BK_0(b\sqrt{q^2+\kappa_D^2})]^{-1}, \tag{5}$$

and K_0 is the zeroth order modified Bessel function of the second kind, which results due to the electrostatic interaction. One notes that in treating the electrostatic energy term in Eq. (1), the unit segment length b is involved as a lowest cutoff length to avoid singularity arising from self-interactions between the charges.

From the equipartition theorem, the average of energy per mode in Eq. (4) has $k_BT/2$ so that

$$\langle|\delta\sigma(q)|^2\rangle = S(q). \tag{6}$$

Since K_0 is positive definite, Eq. (6) shows that the charge fluctuation is restrained by the electrostatic effects. As the electrolyte concentration c increases, the Coulomb interaction is screened so that $S^{-1}(q)$ approaches χ. Furthermore, χ is a decreasing function of z and thus large valency enhances the fluctuation. Including this electrostatic interaction effect, the strength (or the variance) of the density fluctuation $\langle\delta\sigma^2\rangle$ is

$$\langle\delta\sigma^2\rangle = \frac{1}{L}\sum_q\langle|\delta\sigma(q)|^2\rangle = \frac{1}{\pi}\int dqS(q), \tag{7}$$

where q runs from $q_m=\pi/L$ to $q_M=\pi/b$ for the integration. In principle, the cutoff length b can be determined self-consistently by measuring $\langle\delta\sigma^2\rangle$, which is inversely proportional to b in both low-screening and high-screening limits. Since the charge fluctuation in our mesoscopic model originates from the incessant adsorption and desorption of the counterions on the polymer, we take the b as size comparable to the counterions diameter, as discussed later. Figure 1 depicts $\langle\delta\sigma^2\rangle$ as a function of c for three different valences, $z=1$, 2, and 3: it shows that $\langle\delta\sigma^2\rangle$ increases monotonically with c as well as with z. For the value of c smaller than 100 mM, to which the physiological condition applies for $z=1$ case, the variance remains a small constant independent of c. A similar tendency is observed for $z=2$ and $z=3$ and the concentration up to $c\sim 10$ mM. This is the over-riding

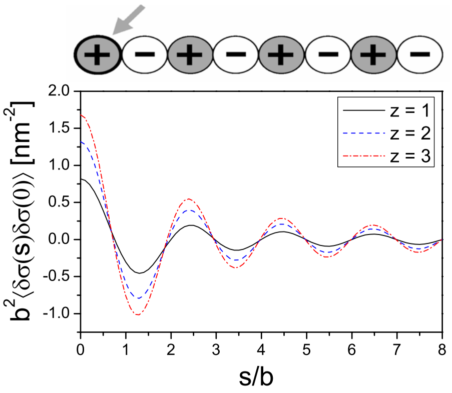

FIG. 2. (Color online) $\langle\delta\sigma(s)\delta\sigma(0)\rangle$ with various z at $c=50$ mM. The correlation functions oscillate with a characteristic length b independent of z, and with the amplitude increasing with z. This behavior can be interpreted by the linear response theory, where the oscillation of the correlations corresponds to distribution of the charge density and coordination of alternating charge in response to a charge placed at $s=0$ (arrow). All the other parameters are the same used in Fig. 1.

effect of the electrostatic interaction by the electrolyte. The counterion-induced enhancement of the fluctuation can be maximal by an interplay of the multivalency and high electrolyte concentration. We here take $a=0.17$ nm, $b=0.4$ nm as the typical hydrated counterion diameter [5,16], $l_B=0.71$ nm for water at 300 K and $L=80$ nm.

We obtain static charge correlation functions by inverse transform of Eq. (6),

$$\langle\delta\sigma(s)\delta\sigma(0)\rangle = \frac{1}{L}\sum_q e^{-iqs}\langle|\delta\sigma(q)|^2\rangle = \frac{1}{2\pi}\int dq e^{-iqs}S(q)$$
$$= \frac{1}{\pi}\int_{\pi/L}^{\pi/b} dq\,\cos(qs)S(q), \tag{8}$$

and the normalized static correlation function

$$C(s) = \langle\delta\sigma(s)\delta\sigma(0)\rangle/\langle\delta\sigma^2\rangle. \tag{9}$$

Figure 2 shows $\langle\delta\sigma(s)\delta\sigma(0)\rangle$ for various values of z with $c=50$ mM. Strikingly, it has an oscillatory behavior with a wavelength $\approx 2b$ for all values of z, but with the amplitude increasing with z. This is understood in part if we consider that

$$C(s) = \frac{\displaystyle\int_{q_m}^{q_M} dq\,\cos(qs)S(q)}{\displaystyle\int_{q_m}^{q_M} dq S(q)}. \tag{10}$$

In the limit of high screening $S(q)=\chi^{-1}$ and $C(s)=\sin(\frac{\pi s}{b})/\frac{\pi s}{b}$. In the other cases, $S(q)$ in Eq. (10), understood as a weighting function, rapidly increases with q, so that $C(s)\sim\cos(\frac{\pi s}{b})$. The oscillation of $\langle\delta\sigma(s)\delta\sigma(0)\rangle$ is characterized by the wavelength $2b$, and the amplitude proportional to z^2 and $\langle\sigma_z\rangle$.

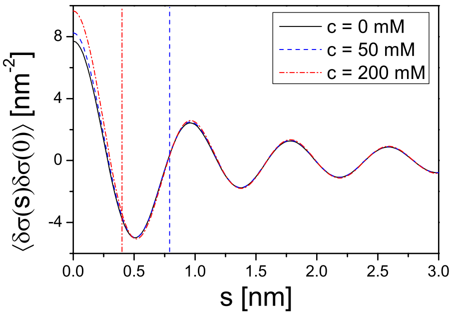

FIG. 3. (Color online) $\langle\delta\sigma(s)\delta\sigma(0)\rangle$ with various c at $z=2$. Variation of the fluctuation is dominantly enhanced within the screening length [vertical lines: 50 mM (dashed blue) and 200 mM (dash-dotted red)]. All the other parameters are the same used in Fig. 1.

To gain an idea about the nature of oscillation physically, consider the linear response theory [23], according to which $\langle\delta\sigma(s)\delta\sigma(0)\rangle$ is proportional to the average of $\delta\sigma(s)$ that occurs in response to charging at $s=0$. The oscillation is attributable to successive coordination of charges in alternating signs in response to this central charge, which is originated from competition between electrostatic attraction and hard-core repulsion [24]. The charging can be done by absorbing counterions which can inverse the negative charge of DNA to a positive value. In the nearest neighborhood of this positive central charge, a negative correlation (negative charge) would appear, leading to electrostatic attraction. The charge oscillation behavior is in accord with the result of Ha *et al.* [5], where the charge oscillation of the static charge correlation along a charged rod with the *unscreened* electrostatic interaction occurs due to the finite size of counterions which they incorporated. Indeed, this type of oscillation of the charge density fluctuation correlation was detected in small angle x-ray scattering experiments in two-phase ionic liquids where the diffusive electron density distribution alternates along one direction [25]. In the scattering experiments, $S(q)$ in Eq. (5) represents the structure factor which is proportional to differential cross sections. Recently, Naji *et al.*, using Monte Carlo simulations [15], reported that the one dimensional pair correlation function of the condensed counterions, which represents the probability distribution of the charge density along the axis, has an oscillatory behavior with its amplitude increasing with z (in their ξ and Ξ).

Figure 3 depicts the correlation function with various electrolyte concentrations with $z=2$. The vertical lines denote the screening lengths for 50 mM (dashed blue) and 200 mM (dash-dotted red), respectively. The amplitude of the correlation is enhanced not only by $c\gtrsim 10$ mM as described above in Fig. 1 but also mainly within the screening length.

III. THE DYNAMIC CORRELATION FUNCTIONS

Dynamics of the charge fluctuation due to condensing counterions is an important issue but poses a challenge to measure nanoscale resolutions in both space and time. Recently, Angelini *et al.* reported liquidlike organization of the condensed counterions (Ba^{2+}, Sr^{2+}, and Mg^{2+}) between attracted F-actin filaments and their acousticlike phonon mode using inelastic x-ray scattering [16]. They found the diffusion coefficient of the condensed counterions with $z=2$ at $c \sim 30$ mM has $\sim 5.0 \times 10^9$ nm^2/s by fitting with a simple Lorentzian structure factor. This diffusion coefficient gives estimation of the counterion "residence time," the time to diffuse a distance equal to its size, to be $\sim 10^{-2}$ ns. Also, molecular dynamics simulation study [18] reported that the condensed counterions with $z=1$ have a short lifetime of order 10^{-1} ns.

Assuming the net charge on the polymer rod is conserved, the charge fluctuation in time is governed by the Cahn-Hilliard diffusion model [24,26],

$$\frac{\partial}{\partial t}\delta\sigma(s,t) = D_o \frac{\partial^2}{\partial s^2}\left(\frac{\delta H}{\delta[\delta\sigma(s)]}\right) + \xi_\sigma(s,t), \tag{11}$$

where D_o is the Onsager coefficient and $\xi_\sigma(s,t)$ is the Gaussian random noise related with the diffusion constant D by the fluctuation-dissipation theorem

$$\langle \xi_\sigma(s,t)\xi_\sigma(s',0)\rangle = -2k_B T D \frac{\partial^2}{\partial s^2}\delta(s-s')\delta(t). \tag{12}$$

From the Fourier transform of Eq. (11), we obtain

$$\frac{\partial}{\partial t}\delta\sigma(q,t) = -D_e q^2\left(\frac{\delta H}{\delta[\delta\sigma^*(q)]}\right) + \xi_\sigma(q,t), \tag{13}$$

which, by substitution of the Hamiltonian in Eq. (4), becomes

$$\frac{\partial}{\partial t}\delta\sigma(q,t) = -D_e(q)q^2\delta\sigma(q) + \xi_\sigma(q,t) = -\frac{\delta\sigma(q)}{\tau_\sigma(q)} + \xi_\sigma(q,t). \tag{14}$$

Here, $D_e(q)=D/\chi S(q)$ is the renormalized diffusion constant while D is the diffusion constant of the counterions without the Coulomb force. Note that $D_e(q) = D[1+2l_B K_0(b\sqrt{q^2+\kappa_D^2})/\chi]$ is larger than D by the fraction $2l_B K_0(b\sqrt{q^2+\kappa_D^2})/\chi$. We take $D \approx 1.2 \times 10^9$ nm^2/s using the Einstein relation $D=k_BT/(3\pi\eta b)$ for 300 K water, and $\tau_\sigma(q)=\chi S(q)/Dq^2$ is the characteristic relaxation time of the charge density fluctuation. From Eq. (14), we find the time correlation function,

$$\langle \delta\sigma(q,t)\delta\sigma^*(q,0)\rangle = \langle |\delta\sigma(q)|^2\rangle e^{-t/\tau_\sigma(q)}, \tag{15}$$

and its inverse transform is

$$\langle \delta\sigma(s,t)\delta\sigma(0,0)\rangle = \frac{1}{\pi}\int dq S(q)\cos(qs)e^{-t/\tau_\sigma(q)}. \tag{16}$$

Figure 4 shows the normalized dynamic correlation function for the charge fluctuation for different times at $z=1$ and $c=100$ mM. Due to the charge diffusion with diffusivity D, the correlation relaxes to zero as time elapses. Like the static correlation functions, the dynamic counterparts also can be interpreted by linear response theory [24]. Retain an excess charge at $s=0$ until it is released at $t=0$. The average charge induced on s at time t is proportional to $\langle \delta\sigma(s,t)\delta\sigma(0,0)\rangle$. The characteristic time can be estimated to have $\tau_\sigma = \chi S(q_M)/(q_M^2 D)$ for the mode of oscillation corresponding to $q_M=\pi/b$. Hence one can estimate the τ_σ, for each $z=1$, 2, and 3 case with their physiological electrolyte concentrations, respectively, to be in the order of 10^{-2} ns, which is in the same order of magnitude observed in the related experiment of Ref. [16].

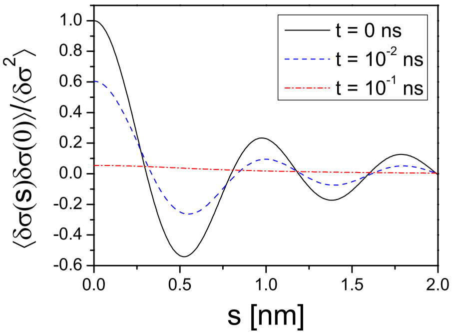

FIG. 4. (Color online) The normalized dynamic correlation function of $\delta\sigma$. $z=1$, $c=100$ mM, $D=1.2\times10^9$ nm^2/s. The characteristic time of decay is of order 10^{-2} ns. We use $a=0.17$ nm, $b=0.4$ nm, $l_B=0.71$ nm, and $L=80$ nm.

The dependence of the dynamic correlation on z is depicted for $z=1$, 2, and 3 at $t=10^{-2}$ ns and $c=50$ mM in Fig. 5. It shows that as z increases, the charge density fluctuation decays faster. Note that the decay of the oscillations occurs within $s \sim 1.4$ nm which is λ_D at $z=1$ and $c=50$ mM.

To characterize the time dependence of the correlation, we consider the autocorrelation function at an equal position,

$$C(t) = \frac{\langle \delta\sigma(s,t)\delta\sigma(s,0)\rangle}{\langle \delta\sigma^2\rangle} = \frac{\displaystyle\int dq S(q)X(q,t)}{\displaystyle\int dq S(q)}, \tag{17}$$

where

$$X(q,t) = e^{-Dq^2 t S(q)^{-1}/\chi}. \tag{18}$$

When there is no electrostatic interaction, Eq. (17), by noting $S(q) \to 1/\chi$, is reduced to

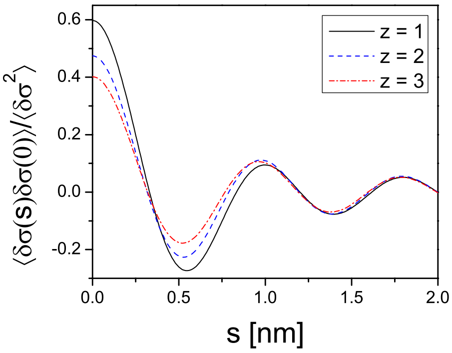

FIG. 5. (Color online) The normalized dynamic correlation function of $\delta\sigma$ with $z=1$, 2, and 3 at $t=10^{-2}$ ns, $c=50$ mM, and $D=1.2\times10^9$ nm^2/s. The decay of the fluctuation is enhanced with z in region $s \lesssim b$. All the other parameters are the same used in Fig. 4.

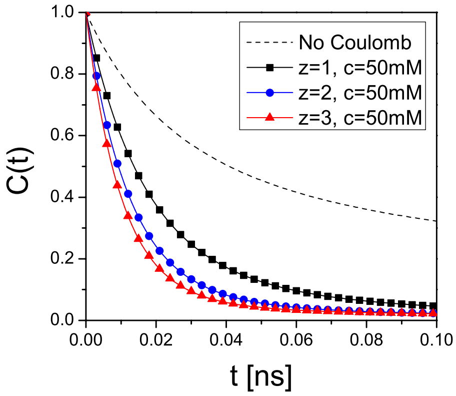

FIG. 6. (Color online) Numerical plot of the normalized autocorrelation functions of the charge fluctuation vs time with various value of $z=1$, 2, and 3 at $c=50$ mM. The dashed black line depicts highly screened limit, i.e., no electrostatic interaction. All the other parameters are the same used in Fig. 4.

$$
\begin{aligned}
C_0(t) &= (q_M - q_m)^{-1}\int_{q_m}^{q_M} dq e^{-Dq^2 t} \\
&= \frac{\sqrt{\pi}}{2}\frac{\mathrm{erf}(\sqrt{Dt}q_M) - \mathrm{erf}(\sqrt{Dt}q_m)}{\sqrt{Dt}(q_M - q_m)}, \qquad (19)
\end{aligned}
$$

where erf denotes the error function. When $b^2/D \ll t \ll L^2/D$, Eq. (19) is reduced to

$$
C_0(t) = \frac{b}{\sqrt{4\pi D t}} \sim t^{-1/2}, \qquad (20)
$$

characteristic of one-dimensional free diffusion. Figure 6 depicts numerical plots of the autocorrelation function in Eq. (17) with $z=1$, 2, and 3 at $c=50$ mM along with $C_0(t)$ in Eq. (19) (the dashed black line). The electrostatic interaction gives the decay of the autocorrelation much faster than in $C_0(t)$, the trend of which is enhanced as z increases.

To explain the electrostatic effect on the autocorrelation, we emphasize that $C(t)$ in Eq. (17) is the average of $X(q,t)$ over all distribution of q weighted by $S(q)$. Since $S(q)$ is a rapidly increasing function up to q_M as noted earlier, $S(q)X(q,t)$ has a maximum at q_0 which is order of q_M, so that $C(t)$ can be approximated as

$$
\begin{aligned}
C(t) &\approx X(q_0,t) \\
&= e^{-Dq_0^2 t S(q_0)^{-1}/\chi} \\
&= \exp\{-Dq_0^2 t[1 + 2(\xi - 1)K_0(b\sqrt{q_0^2 + \kappa_D^2})]\} \\
&= \exp\{-Dq_0^2 t[1 + \alpha(q_0,z,c)]\}. \qquad (21)
\end{aligned}
$$

$\xi = z l_B/a$ is the Manning parameter: when $\xi > 1$, counterion condensation occurs. The $\alpha(q,z,c) = 2(\xi - 1)K_0(b\sqrt{q^2 + \kappa_D^2})$ denotes the fraction of diffusivity enhancement by electrostatic effect due to the counterions. Figure 7 shows comparison of the approximated correlation functions (dotted lines) in Eq. (21) with $C(t)$ in Fig. 6 (solid lines) around the characteristic time, 0.1 ns. They are in good agreement with q_0 of order of q_M, $q_0=0.54q_M$ (no Coulomb), $0.63q_M(z=1)$, $0.59q_M(z=2)$, and $0.53q_M(z=3)$, respectively.

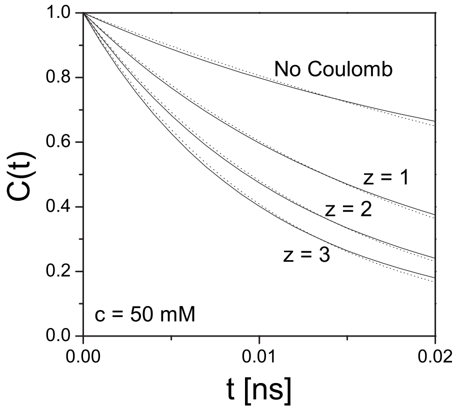

FIG. 7. Comparison of the approximated $C(t)$ (dotted lines) with Fig. 6 (solid lines) around the characteristic time, 0.1 ns. we take $q_0=0.54q_M$ (no Coulomb), $0.63q_M(z=1)$, $0.59q_M(z=2)$, and $0.53q_M(z=3)$, respectively.

On the other hand, considering c dependence of the autocorrelation, the $\alpha(q,z,c)$ is a decreasing function of c, and $C(t)$ decays more slowly as c increases at fixed z. Figure 8 depicts the numerical plot of the autocorrelation in Eq. (17) with $c=10$, 100, and 500 mM at $z=1$. Note that our approximated $C(t)$ in Eq. (21), in the same manner of the above z dependence case, well describes this tendency of the decay with c. This implies that as screening length is shortened to b, the interaction between the effective charges on the polymer is screened so much that they seldom respond to the perturbation (removed charge at $s=0$) and the $C(t)$ eventually decays more slowly than that of more strongly interacting (low c) ones. Note that increase of the electrolyte concentration enhances the local charge fluctuation within the screening length (in the static correlation) but slows its decay (in the dynamic correlation).

IV. SUMMARY

We have investigated static distribution and dynamic relaxation of the charge density along a rodlike polyelectrolyte

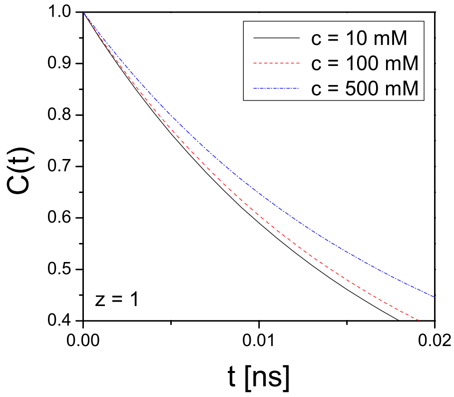

FIG. 8. (Color online) Numerical plot of the normalized autocorrelation functions of the charge fluctuation vs time with various values of $c=10$, 100, and 500 mM at $z=1$. All the other parameters are the same used in Fig. 6.

in an ionic solution from the charge correlation functions. Due to the counterions adsorbed on the negative charged rod, the charge density fluctuates with the electrostatic interaction screened by the electrolyte. We found that the charge density correlation along the rod has an underdamped oscillatory behavior. This was interpreted as the charge distribution induced as response to a central charge perturbation, in accordance with the linear response theory. The length period of the oscillation is directly related to the lower cutoff length b, which is ascribed to the hard-core size of the counterions adsorbed. It is shown that as multivalency z and ionic concentration c increase, the amplitude of the static correlation function increases due to fluctuation and screening of charges, while the period of oscillation is nearly independent of z and c. This oscillatory behavior of the charge fluctuation has been already found in the two phase diffusive ionic liquid system [25] and confirmed by theory [5], numerical simulation [14,15], and experiment [8].

In dynamical correlations, the decay of the oscillation to the mean charge density gets faster with increasing z as a result of electrostatic effect dominant over the entropic (fluctuational) effect. On the other hand, the decay gets slower with increasing c because, also by the linear response theory, the electrostatic interaction on the polymer is screened so much that the charge density decay in response to the removal of central charge becomes slow down to the free one dimensional diffusion process.

We have studied the charge fluctuation on a charged rodlike polymer with mesoscopic Hamiltonian within the Gaussian level and Manning-Oosawa theory of counterion condensation. Despite its simplicity, our model predicts, as effects of the charge fluctuation and screened electrostatic interaction, one dimensional ionic liquidlike spatial correlation and unusually fast relaxation of the charge density.

ACKNOWLEDGMENTS

This work was supported by Brain-Korea 21 program and SBD-NCRC.

[1] G. S. Manning, J. Chem. Phys. **51**, 924 (1969).
[2] F. Oosawa, *Polyelectrolytes* (Marcel Dekker, New York, 1971).
[3] J. L. Barrat and J. F. Joanny, Adv. Chem. Phys. **79**, 1289 (1997).
[4] R. Podgornik and V. A. Parsegian, Phys. Rev. Lett. **80**, 1560 (1998).
[5] B.-Y. Ha and A. J. Liu, Phys. Rev. E **58**, 6281 (1998).
[6] V. A. Bloomfield, Biopolymers **44**, 269 (1997).
[7] J. Tang, T. Ito, T. Tao, P. Traub, and P. Janmey, Biochemistry **36**, 12600 (1997).
[8] T. E. Angelini, H. Liang, W. Wriggers, and G. C. L. Wong, Proc. Natl. Acad. Sci. U.S.A. **100**, 8634 (2003).
[9] O. V. Zribi, H. Kyung, R. Golestanian, T. B. Liverpool, and G. C. L. Wong, Phys. Rev. E **73**, 031911 (2006).
[10] V. A. Bloomfield, Biopolymers **31**, 1471 (1991).
[11] K. Betesman, K. Van Eijk, and S. Lemay, Nat. Phys. **3**, 641 (2007).
[12] R. Golestanian and T. B. Liverpool, Phys. Rev. E **66**, 051802 (2002).
[13] B.-Y. Ha and D. Thirumalai, Macromolecules **36**, 9658 (2003).
[14] T. Iwaki, C.-Y. Shew, and G. Gumbs, J. Chem. Phys. **123**, 124712 (2005).
[15] A. Naji and R. R. Netz, Phys. Rev. E **73**, 056105 (2006).
[16] T. E. Angelini, R. Golestanian, R. H. Coridan, J. C. Butler, A. Beraud, M. Krisch, H. Sinn, K. S. Schweizer, and G. C. L. Wong, Proc. Natl. Acad. Sci. U.S.A. **103**, 7962 (2006).
[17] L. L. Van Zandt and V. K. Saxena, Phys. Rev. Lett. **61**, 1788 (1988).
[18] T. S. Lo, B. Khusid, and J. Koplik, Phys. Rev. Lett. **100**, 128301 (2008).
[19] J. Barrat and J. Hansen, *Basic Concepts for Simple and Complex Liquids* (Cambridge University Press, Cambridge, England, 2003).
[20] G. Ariel and D. Andelman, Phys. Rev. E **67**, 011805 (2003).
[21] G. S. Manning, Biophys. Chem. **7**, 95 (1977).
[22] G. S. Manning, Acc. Chem. Res. **12**, 443 (1979).
[23] R. Kubo, M. Toda, and N. Hashitsume, *Statistical Physics II* (Springer, Berlin, 1998).
[24] W. Sung, E. Choi, and Y. W. Kim, Phys. Rev. E **74**, 031907 (2006).
[25] G. Strobl, *The Physics of Polymers* (Springer, Berlin, 1996).
[26] P. M. Chaikin and T. C. Lubensky, *Principles of Condensed Matter Physics* (Cambridge University Press, Cambridge, England, 1995).